

Quantifying the daily harvest of fermentation products from the human gut microbiota

Markus Arnoldini^{1,2}, Richa Sharma^{2,*}, Claudia Moresi^{1,*}, Griffin Chure², Julien Chabrey¹, Emma Slack¹, Jonas Cremer^{2,2}

¹ Department of Health Science and Technology, ETH Zürich, Zürich, Switzerland

² Department of Biology, Stanford University, Stanford CA, USA

* Contributed equally

markus.arnoldini@hest.ethz.ch, jbcremer@stanford.edu

Abstract

Fermentation products released by the gut microbiota provide energy and important regulatory functions for the host. Yet, little quantitative information is available on the metabolite exchange between the microbiota and the human host, and thus the effective doses of fermentation products. Here, we introduce an integrative framework combining experimental characterization of major gut bacteria with a quantitative analysis of human digestive physiology to put numbers on this exchange and its dependence on diet and microbiota composition. From the carbohydrates fueling microbiota growth, we find most carbon ends up in fermentation products which are largely utilized by the host. This harvest varies strongly with diet, from between 100-700 mmol/day within the US population to up to 1300 for the Hadza people of Tanzania. Accordingly, fermentation products cover between 1.8% and 12.1% of the daily energy demand of human hosts, substantially less than the 21% estimated for laboratory mice. In contrast, microbiota composition has little impact on the total daily harvest but determines the harvest of specific fermentation products. Butyrate, known for promoting epithelial health, shows the biggest variation. Our framework thus identifies and quantifies major factors driving the metabolic and signaling interactions between microbiota and host, crucial to mechanistically dissect the role of the microbiota in health and disease.

Introduction

The exchange of fermentation products (FPs; mostly acetate, propionate, and butyrate) is a major avenue for the gut microbiota to exert its effects on the host (1, 2). These molecules are excreted by anaerobically growing microbes in the large intestine which feed mostly on complex carbohydrates, such as dietary fiber and resistant starches. Microbial FPs are absorbed by the colonic epithelium and perform a variety of important functions in the host. For example, they serve as energy source (3, 4), influence immune cell regulation and recruitment (5–7), and have a role in satiety signaling (8, 9) and the gut brain axis more generally (1, 10). By changing the pH in the gut lumen, they also allow gut microbes to shape their local environment with strong effects on microbiota composition (11, 12).

FP concentrations have been measured in feces and within the human digestive tract (13, 14). However, these concentrations are the result of a highly dynamic interplay between microbial FP production and uptake by the host which varies strongly with changes in the host's food intake and digestion activity throughout the day (15, 16). Therefore, concentration measurements in gut content are only snapshots and provide little insight into the overall flux of FPs that microbes produce and that the human body takes up.

Here, we integrate our own experimental measurements of bacterial fermentation with a quantitative analysis of human digestive physiology to estimate the daily amount of FPs the gut microbiota provides to the human host. With this framework, we analyze the variation of the daily FP harvest and its contribution to the host's energy demand, depending on diet and microbiome composition.

Results

Quantifying fermentative metabolism of major gut bacteria

To maintain their redox balance and generate energy in the anoxic environment of the large intestine, gut bacteria utilize different fermentation pathways which mostly produce the acids of acetate, propionate, butyrate, lactate, formate, and succinate (**Figure 1A, SI Text 1**). To quantify the production of these FPs and the consumption of carbohydrates, we grew selected gut bacteria in pure cultures and tracked changes in metabolite concentrations and bacterial biomass over time. Metabolite concentrations changed linearly with biomass during steady-state growth, allowing us to determine the per biomass uptake and excretion rates with high precision (**Figures 1B and S1, Methods**).

We picked sixteen gut microbiota species (**Figure 1C and Table S1**) based on their relative abundances in metagenomic data (17, 18). While hundreds of species are typically detectable in a healthy human gut microbiome, abundances are highly uneven and the sixteen species we chose commonly account for close to 60% of total bacterial biomass in the human gut (**Figure S2**). When using these species as representatives of their respective families (**SI Text 1**), coverage increases even to around 90% of biomass (**Figures 1C, S2**). For growth in rich but carbon-limited medium (YCA), uptake of glucose or maltose varied in a relatively narrow range (**Figure 1D; SI Text 2**), in line with the idea that different bacterial strains need similar amounts of carbohydrates to sustain growth (**SI Text 1**). Types of secreted FPs, however, varied substantially between different bacterial species, in line with their metabolic pathways (**Figure 1E**). For example, *Bacteroides* strains excrete succinate and *Lachnospiraceae* produce butyrate (**SI Text 1**). Considering the fate of carbohydrate-derived carbon, we find that most ends up in FPs (**Figure 1F**), illustrating the high demand for carbohydrates required for fermentative growth. We further repeated these experiments in other media of different complexities (BHI, ϵ , and γ media) (**Figure 1G**). Carbohydrate uptake and FP excretion rates are comparable if peptides are available (YCA, BHIS, ϵ), but uptake increases in minimal medium (γ), reflecting the increased carbon demand for biomass synthesis (**Figure S3**). In the analysis following in the main text, we use uptake and excretion rates measured in YCA medium.

In summary, we quantified the per biomass carbohydrate consumption and FP excretion rates of highly abundant gut bacteria that comprise the bulk of the gut microbiota in a healthy human.

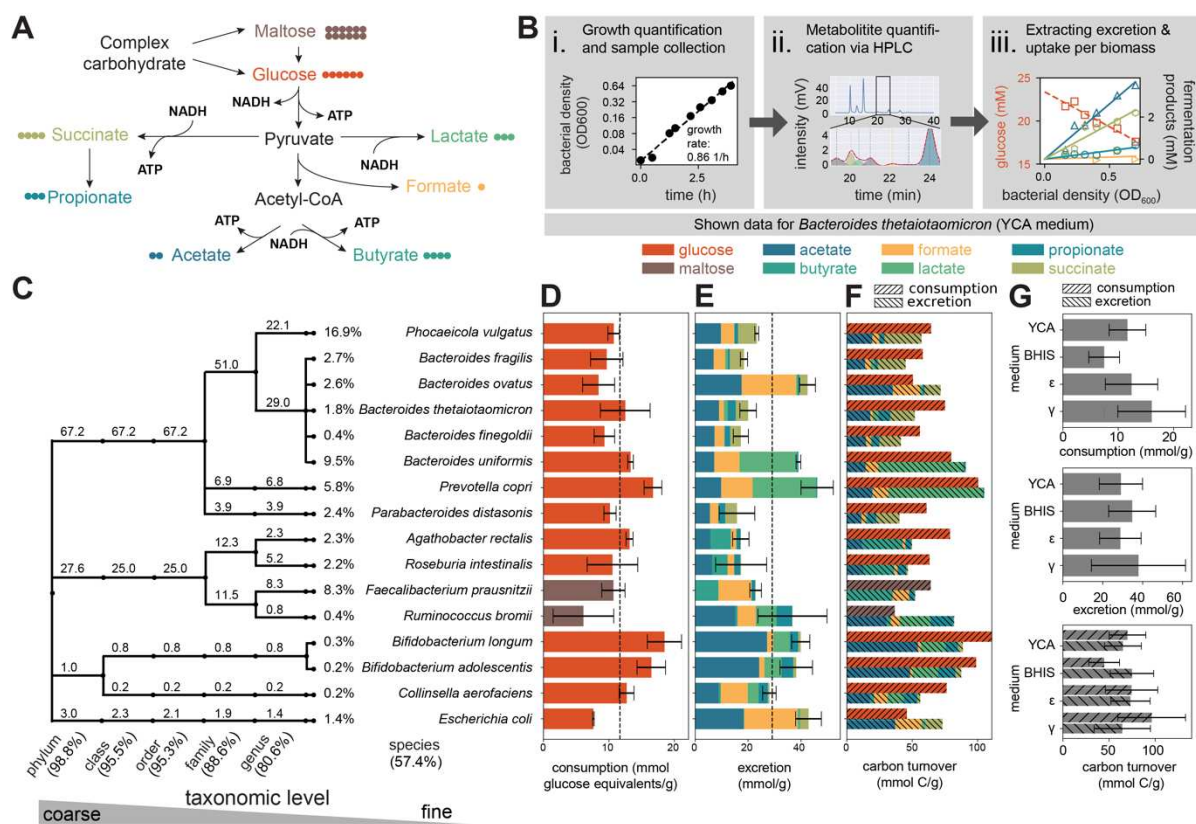


Figure 1. Growth, nutrient uptake, and FP excretion of major gut strains. **(A)** Major fermentation pathways that promote energy synthesis (ATP) and ensure redox balance during anaerobic growth. Colored circles indicate the number of carbon atoms in the corresponding molecules (details on metabolism with full stoichiometry in **SI Text 1**). **(B)** Experimental setup to determine nutrient uptake and FP release. Samples taken at multiple time points throughout steady exponential growth (i) were analyzed for metabolite concentration using liquid chromatography (ii). With this data, we calculated linear concentration trends with bacterial density (iii) to quantify per biomass uptake and excretion. Further details in **Figure S1**. **(C)** Taxonomic classification of the 16 gut microbiota species characterized. Numbers indicate the typical fraction of bacterial biomass these species and their taxonomic groups represent in healthy individuals (samples from (17, 18)). **(D,E)** Per biomass glucose/maltose uptake and FP excretion for growth in YCA medium. Error bars denote SD of three biological replicates. Dashed lines indicate averages of all measured species. **(F)** Carbon content in taken-up carbohydrates and excreted fermentation products. Mismatched carbon balances for *E. coli* and *R. bromii* likely reflect utilization of other media components, such as amino acids, as carbon sources. **(G)** Species averaged uptake and excretion rates in different media (YCA, BHIS, ϵ , γ). Error bars denote SD of species-to-species variation.

Point estimates of the daily FP harvest

Integrating our experimental dataset and a quantitative analysis of diet and digestion, we next estimated the daily amount of FPs released by the gut microbiota in two different ways. To do so, we consider people from 1970's Britain since dietary and digestion data needed for our estimation is available for this cohort in unparalleled quality. First, we estimated the FP release based on fecal weight, following the logic presented in (19) (**Figure 2A and SI Text 3.1**). In the British reference scenario, humans excrete around 30g of fecal dry weight every day (20) (**Figure 2A(i)**, **Figure S4**) of which around 16g is bacterial biomass (21) (**Figure 2A(ii)**). To maintain a stable microbiota in the gut, this loss of bacterial biomass must be compensated by bacterial growth. Using the measured amount of FPs which bacteria release to support growth (29 mmol/g, **Figure 1E**, dashed line), we get a daily production of FPs of approximately

$16\text{g/day} \times 29\text{mmol/g} = 464\text{mmol/day}$ (**Figure 2A(iii)**). Second, we estimated the FP release based on the amount of carbohydrates in the diet (**Figure 2B, C and SI Text 3.2**). From the amount of fiber, sugar, and other carbohydrates in the diet and their digestibility, we estimated the amount of carbohydrates reaching the large intestine (**SI Text 4**). For the British reference scenario, 36g (corresponding to 198mmol equivalents of glucose) of these microbiota-available carbohydrates (MAC) reach the large intestine (22) (**Figure 2B**, with exact values depending on the starch and fiber content in the diet (**Figure S5, SI Text 4**). Using the measured amount of carbohydrate consumption per biomass (12mmol/g, **Figure 1D**, dashed line) approximately $198\text{mmol} / 12\text{mmol/g} = 17\text{g}$ bacterial biomass are produced per day (**Figure 2C(ii)**), leading to a daily FP release of $17\text{g} \times 29\text{mmol/g} = 493\text{mmol}$ (**Figure 2C(iii)**), in good agreement with the estimation via fecal weight.

Given the high carbohydrate demand of anaerobic growth (**Figure 1F**), most of the carbon from MACs will end up in FPs (**Figure 2D**). In contrast, following fecal FP measurements (23), less than 2% of released FPs exit the host via feces (**Figure 2D, SI Text 5**). As the consumption of FPs via cross-feeding is likely limited (**SI Text 5**), the daily amount of FPs released by bacteria represents a good upper bound for the daily amount absorbed by the gut epithelium and thus the daily FP harvest by the human host.

Variation in total FP harvest with changing microbiota composition

The presented point estimates for the daily FP harvest rely on average metabolite consumption and production rates for 16 highly abundant gut microbiota members. However, gut microbiota composition can vary considerably (24). For example, the relative abundance of primary fermenters from the families Bacteroidaceae and Lachnospiraceae varies considerably between healthy individuals (**Figure 3A**, upper panel). To assess the effect of these changes in microbiota composition on FP harvest, we weighted measured consumption and production rates of different species with their relative abundance, using them as metabolic representatives of their respective families (**Figure S6, SI Text 6**). Assuming MACs corresponding to the British reference diet, the relative amount of different FPs released varies substantially between individuals (**Figures 3A** lower panel, and **B**). However, both the daily production of bacterial biomass (**Figure 3C**) and the total daily release of FP (**Figure 3D**) remain within a narrow range. These differences in variation are quantified by the coefficients of variation (**Figure 3E**), with butyrate showing the highest value. Changes in FP release with host age, health, and lifestyle, obtained from a collection of published metagenomic data (25), can be explored in the **Interactive Figure 1** (https://cremerlab.github.io/fermentation_products/study-explorer) accompanying this paper.

In summary, this analysis shows that, given a specific diet, differences in microbiota composition lead to differences in the types of FPs released, while the total daily release of FP remains within a narrow range.

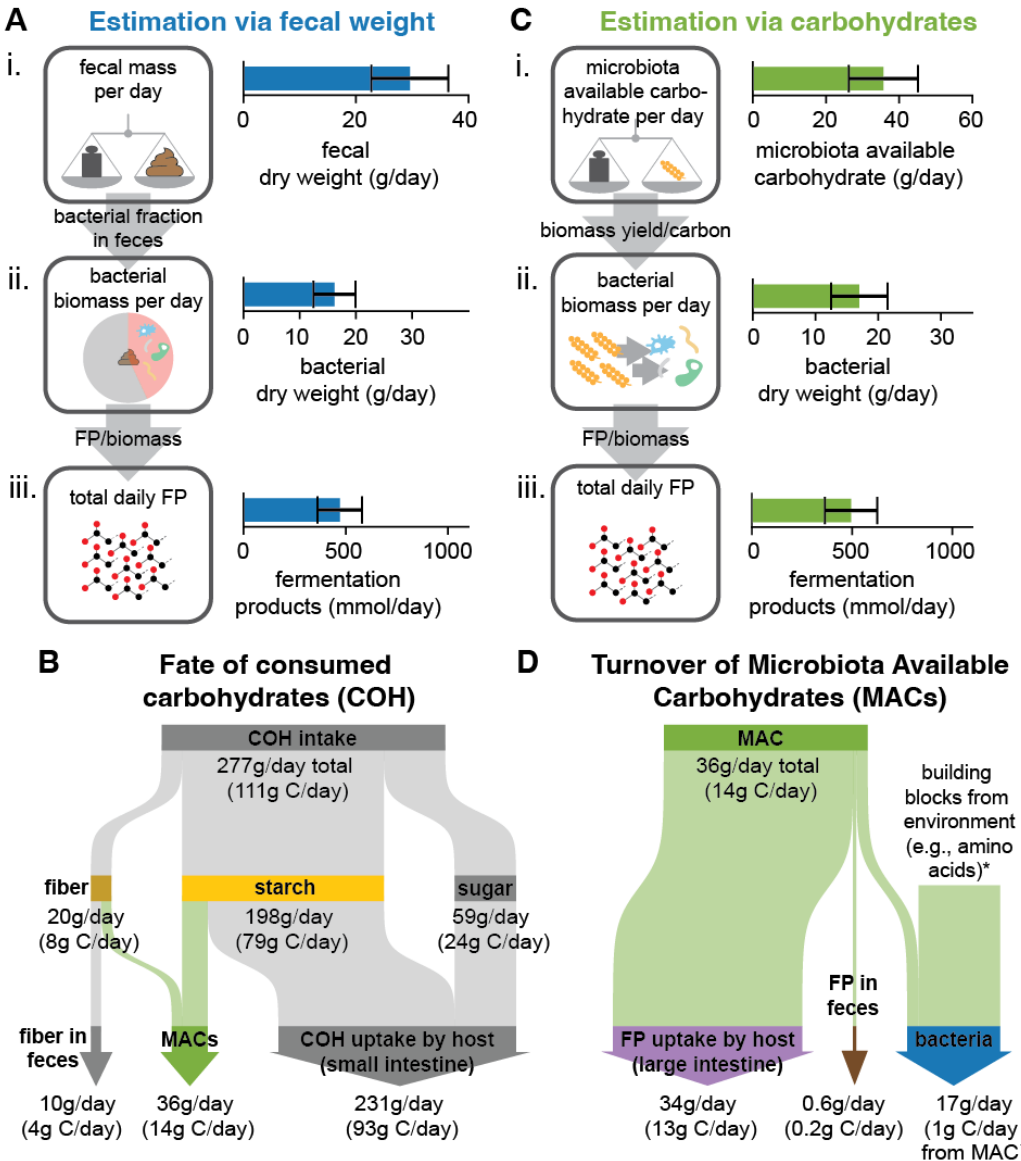


Figure 2. Daily FP harvest for British reference scenario. (A) Fecal-weight-based point estimate of the total daily FP release. Starting point is the measurement of daily fecal weight (20) (i). Given the fraction of bacteria in fecal weight (21), bacterial biomass in feces follows (ii) which, given the measured FP excretion, sets the total daily FP production (iii). (B) Flow diagram showing the daily turnover of consumed carbohydrates along the upper digestive tract with only a fraction being available for the microbiota (details of this mapping described in **SI Text 4**). (C) Carbohydrate-based point estimate of the total daily FP release. Starting point is the estimation of microbiota available carbohydrates (i). With experimentally determined uptake and excretion rates (**Figure 1**), it follows the bacterial biomass that gut bacteria synthesize (ii) and the resulting FP harvest when bacteria grow on these carbohydrates (iii). (D) Flow diagram showing resulting carbohydrate and carbon flow along the large intestine, with most of the carbon ending up in FPs that are absorbed by the host. Calculations are based on species-averaged uptake and excretion rates (**Table S2**) obtained from our growth characterization of major gut species (**Figure 1**). g C/day of total carbohydrates, fiber, starch, sugar, and MAC were calculated by assuming a fraction of carbon per total weight equal to glucose (0.4); the fraction of carbon in bacterial biomass was taken to be 0.39, based on data in (26). Error bars in A and C denote SD based on the variation in daily fecal weight and MACs, respectively. Detailed calculations are described in **SI Text 3**.

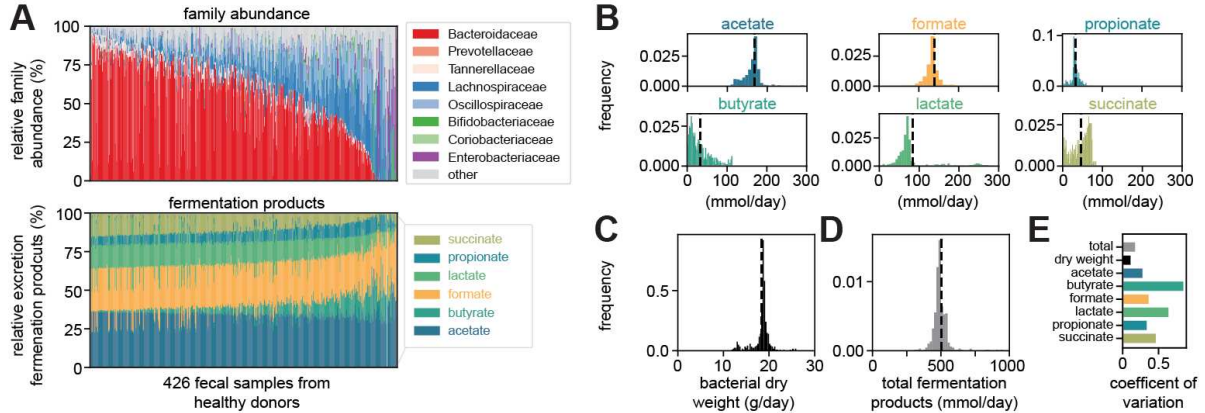


Figure 3. The effect of microbiota composition on daily FP harvest. (A) Variation of gut microbiota composition on the family level (top) and corresponding molar fraction of different fermentation products (bottom) across fecal samples from healthy individuals (17, 18). (B,C,D) Distribution of the daily release of single FPs (B), total bacterial biomass (C), and total amount of fermentation products (D) for the same set of samples. (E) Coefficients of variation quantify these variations, with the variation in total FP release being much smaller than variations in the production of specific FPs. Estimations assume carbohydrate consumption as for the 1970's British reference scenario (Figure 2BC). Details of calculations introduced in **SI Text 6**. The variation with carbohydrate consumption and for further datasets on microbiota composition can be explored in **Interactive Figure 1**.

Variation in total FP harvest with changing diet

To quantify the variation in daily FP harvest with diet, we next analyzed data on diet composition and digestion from three different cohorts, covering much of the global variation in human diets.

First, we estimated the variation in the US population using nutrition data from the 2017/2018 National Health and Nutrition Examination Survey (NHANES) study (27) (Figure S7A-F). Using the same mapping as above (Figure 2B, **SI Text 4**), we inferred daily MAC intake in this cohort (Figure S8A-C) and estimated FP harvest based on these values (Figure 4A), with constant uptake and excretion characteristics given by the averages of the experimentally characterized species (Figure 1DE, dashed lines). The FP harvest is broadly distributed around a mean of 340mmol/day, with most individuals staying substantially below the estimate for the British reference scenario (Figure 4A, purple dashed line), reflecting how modern western diets lead to less FP harvest from the gut microbiota (28–30).

Second, we analyzed nutrition data available for the Hadza, an indigenous hunter-gatherer group in Tanzania. Their diet, including the amount of carbohydrates consumed, differs substantially from a modern western diet, has strong seasonal variation, and often includes fiber-rich tubers (31, 32) (Figure S7G, H). Accordingly, the estimated amount of MACs (Figure S8D-F) and the resulting daily FP harvest show strong seasonal variation (Figure 4B, **SI Text 4**). Harvests are much higher than those typically observed for people consuming western diets and can reach up to 1280mmol/day.

Third, we estimated the global variation in FP harvest based on fecal weight data representing different geographical regions and lifestyles around 1970 (33). Daily excretion of fecal wet weight varies strongly, with maximum values about five times higher than in the British cohort (Figure S9A). Correcting for changes in water content with fecal mass (14, 21, 34–38) and assuming a constant bacterial fraction per fecal dry weight (Figure S9), we estimated the corresponding variation in FP harvest (Figure 4C). As differences in fecal weight are largely

due to differences in diet (34, 38, 39), this broad variation with a maximum value of 1500 mol/day again emphasizes the importance of diet for daily FP harvest.

In summary, we quantified how variation in diet determines FP harvest, and find that diet, and not microbiota composition, is the dominant factor in setting this number. Particularly, we estimate how diets low in MACs, as consumed in the US and increasingly around the globe, exhibit much lower FP yields than fiber-rich diets with potentially detrimental health outcomes (28–30).

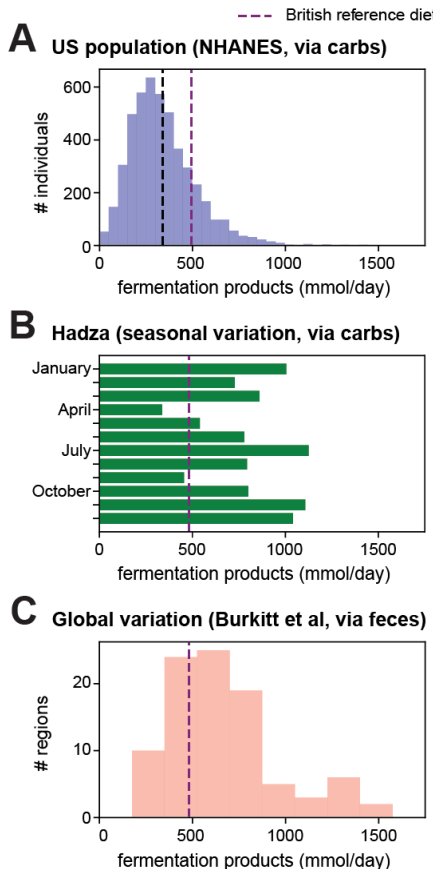


Figure 4. Variation of the daily FP harvest with diet and digestion. (A) Inter-individual variation in total daily FP production for the US population. Carbohydrate-based estimate using reported variation in diet for the NHANES 2017/2018 cohort (27). (B) Month-to-month variation of total daily FP production for the Hadza. Carbohydrate-based estimate using reported seasonal variation in diet (31). (C) Variation in FP production based on fecal-based estimate and global variation in fecal weight reported in Burkitt et al (33). These numbers represent an upper bound estimation (Figure S9 for detailed discussion). Estimates in this figure are based on average per-biomass uptake and excretion rates for the 16 strains characterized in Figure 1.

Gut microbiota derived FPs as energy source for the host

We next compared the human FP harvest with that of the mouse, the most common experimental model in gut microbiota research. Hoces and co-workers have recently compared the energy extraction from food in germ-free and conventionally colonized mice (16). Energy extraction is lower by 8.1 kJ/day in germ-free mice (Figure 5A,B), likely due to a lack of MAC-derived FPs that serve as energy sources for the host (SI Text 8.1). When estimating the harvest of FPs (via fecal weight, analogous to Figure 2A) and their energy content (*i.e.*, combustion enthalpy, see SI Text 7) for these mice, we find that FPs can explain

this difference in energy extraction (**Figure 5C, SI Text 8.2**), indicating that most FPs are utilized as an energy source by the host. In the same way, we calculated the energy content of the FP harvest in humans. Depending on diet and digestion (**Figure 4**), these values vary between 0.1MJ/day and 1.2 MJ/day. To put these numbers into perspective and allow a comparison with values in mice, we normalized them by the daily energy expenditure of the respective host (approximately 10MJ/day for humans (40) and 38kJ/day for mice (16), **SI Text 7**). For the British reference scenario, the gut microbiota contributes 4.4±1.1% of the host's daily energy expenditure (**Figure 6**, purple dashed line). We find broad variation around this number, with values varying from 1.8% (5th percentile of the NHANES cohort, **Figure 6**, blue) to 12.1% in the extreme cases of non-western diets (**Figure 6**, red; 95th percentile from Burkitt data). In contrast, for mice we arrive at 21.4% or more of the total energy demand of 38kJ/day (16) (**Figure 6**, grey, and **SI Text 8**). Notably, these mice were fed autoclaved laboratory chow, and mice consuming non-autoclaved food or a more natural diet are likely to consume more microbiota-available carbohydrates, resulting in an even higher microbiota derived energy supply (41). Therefore, our analysis reveals and quantifies a substantial difference in microbiota-supplied energy between humans and mice.

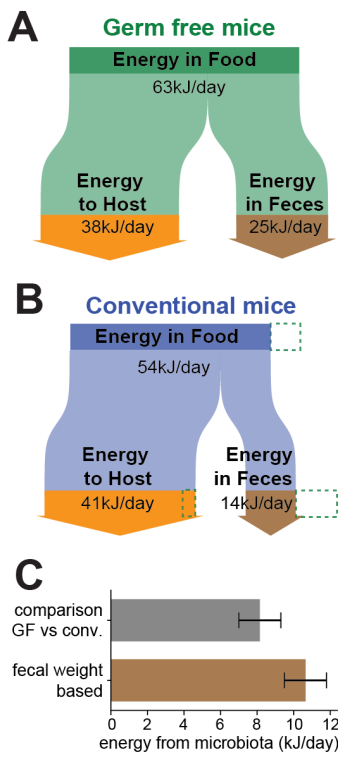


Figure 5. Daily metabolic energy contribution of the gut microbiota in mice. (A, B) Flow charts illustrate the flow of the energy consumed as food in germ-free (A) and conventionally colonized mice (B). Around 60% or 75% of the consumed energy is retained in Germ-free and conventionally colonized mice, respectively. The rest is excreted in feces. Accordingly, the energy consumed in food and energy in feces is lower in conventional mice, while the energy retained in the host is only slightly higher. Green dashed lines in B indicate these differences. **(C)** Daily host energy provided by the gut microbiota when comparing the energy retention in germ-free and conventional mice (upper bar) or when estimating FP production using fecal mass in mice (lower bar, analogous to **Figure 2A**). Error bars denote SD based on the variation of consumed food and fecal weight of different mice (upper estimation). Based on data reported in (16).

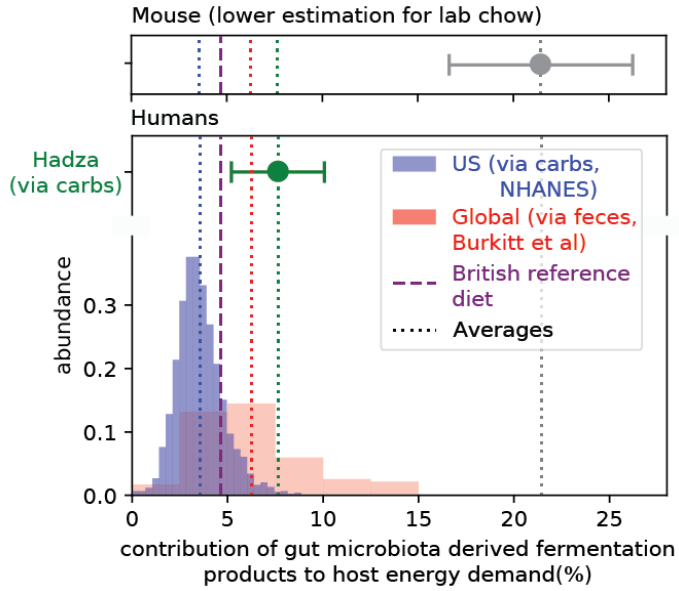


Figure 6. Microbiota contribution to energy supply. Variation of FP harvest leads to strong variation in the fraction of daily energy demand supplied by the gut microbiota. Non-western diets show substantially higher values (green, red), with an upper bound estimation of 15%, when compared to a cohort of US residents (blue). Laboratory mice feeding on autoclaved lab chow (grey) show a substantially higher percentage of daily energy covered by the microbiota. We expect values in mice to be even higher when they consume non-autoclaved food reflecting their natural diet. Error bars indicate variation (SD) based on monthly variation in food intake (Hadza data, green, based on data in (31)), and on error propagation using data originally published in (16) (mouse data, gray, see **SI Text 8.2**), respectively,

Discussion

Recent studies have emphasized the importance of quantitative physiological considerations in microbiome research (11, 42, 43). By integrating data on nutrient intake and fecal mass with experimental measurements of bacterial growth and fermentation rates, we quantified the daily turnover of bacterial biomass and the fermentation product harvest in the human intestine.

We performed complementary analyses that led to similar outcomes, confirming the validity of our integrative framework. First, the FP harvest is highly comparable when deriving it from consumed carbohydrates or released feces, both for the point estimate of the British reference scenario and when analyzing its variation (**Figures 2D and 4**). Second, a theoretical consideration based on the ATP turnover required to generate bacterial biomass predicts a similar total FP harvest for the British reference scenario (19) (**SI Text 3.3**). Third, estimating FP harvests via fecal weight matches an analysis of energy extraction by the microbiota in mice (**Figure 5C**).

When utilizing this framework to analyze FP harvest, several findings stand out. The bulk of carbon in microbiota available carbohydrates, >90%, ends up in fermentation products, most of which are taken up by the host (**Figure 2D**). Quantitatively, FPs thus dominate the metabolite exchange between the microbiota and the host, affecting host signaling, behavior, and energy homeostasis. They are thus a factor which should always be included in studies of host-microbiota interactions. Differences in the total FP harvest is primarily determined by variation in diet, with higher FP harvests resulting from the consumption of less processed foods rich in complex carbohydrates. In contrast, microbiota composition has less impact on

the total daily FP harvest. However, microbiota composition strongly impacts the harvest of specific fermentation products, with butyrate and lactate showing the strongest dependence on composition (**Figure 3E**). Given the different ways specific FPs affect host processes (44), this finding may underlie many of the commonly reported links between health status and microbiota composition, even without explicitly considering the dominant effect of diet on total FP harvest. However, as dietary changes also cause changes in microbiota composition (45), diet is likely the key determinant for both, the abundance of specific FPs and the total FP harvest. Thus, our results highlight that the axis between diet, microbiota composition and FP harvest should routinely be considered when investigating host-microbiota interactions, their role in host health, and the etiology and progression of different microbiota-associated diseases. Critically, we demonstrate that FPs measured in feces represent only a small fraction of the total production, which should rather be estimated using our integrative framework based on diet and microbiome composition.

Our analysis also reveals an important systemic difference between humans and mice. Specifically, the FP harvest per body weight is much higher in mice than in humans (approximately 393 mmol/kg/day for the mouse vs. 7 mmol/kg/day for humans, **SI Text 8.3**). This difference is also reflected in the contribution of microbiota-derived FPs to the daily energy demand, which is much higher in mice compared to humans (1.8-12.1% in humans vs 21.4 % in laboratory mice, **Figure 6**). Together with previously reported differences in microbiome composition and anatomy of the digestive tract (46-50), this difference in FP harvest needs to be accounted for when utilizing mouse studies to explore possible systemic effects of the microbiota on the human host. For example, while specific microbiota perturbations have strong physiological and behavioral effects in mice, comparable perturbations in humans might have a smaller impact (51), simply because mice rely more on FP-derived energy than humans. On the other hand, local characteristics like the absorption of FP per epithelial surface area might be more comparable (171 and 233 mmol/m²/day in mice and humans, respectively; **SI Text 8.3**), suggesting that local interactions between the human microbiota and the intestinal mucosa can be emulated more realistically in mouse studies.

More generally, this study emphasizes the strong potential of quantitative analyses that incorporate microbial metabolism, diet, host physiology, and microbiota turnover to put numbers on the metabolic exchange between microbiota and host. By providing information on specific doses, this goes well beyond the identification of microbiota-derived molecules and their possible interactions with the host. Besides the quantification of major fermentation products and their harvest in this study, many other interaction paths would benefit from such an integrative analysis. This includes the nitrogen cycling between the host and the gut microbiota (52), the role of cross-feeding in the exchange of gases such as H₂ (53) and CO₂, and the microbial digestion of proteins which exposes the host to branched-chained fatty acids and toxic waste products like hydrogen sulfide. In the context of the dynamic, flowing environment of the intestine (54), developing such frameworks is critical to move the field away from misleading assumptions based on point measurements of metabolite concentrations towards an integrated model of host-microbiome functions driving health and disease.

Methods

Bacterial strains and culturing conditions. All characterized strains were obtained from established strain repositories and are listed in **Table S1**. Details for all media components and laboratory supplies are listed in **Table S5**. Bacteria were grown in the media indicated in the respective figures. BHIS medium is Brain Heart Infusion supplemented with 10mg/L hemin (prepared as in (55)) and 1g/L L-cysteine. YCA medium is a modified version of YCFA (56), containing 1% casitone 0.25% yeast extract, 0.1% meat extract, 4g/L NaHCO₃, 1g/L cysteine, 0.45g/L K₂HPO₄, 0.45g/L KH₂PO₄, 0.9g/L NaCl, 0.09g/l MgSO₄•7 H₂O, 0.12 g/L CaCl₂•2H₂O, 10mg/L hemin, 0.02mg/L cobalamin, 0.06mg/L p-aminobenzoic acid, 2mL/L BME vitamins, 10mM sodium acetate, 20mM NH₄Cl, and 20mM glucose or 10mM maltose, respectively. Gamma medium is a fully defined medium, containing 72mM K₂HPO₄, 28mM KH₂PO₄, 50mM NaCl, 0.5mM CaCl₂, 0.4mM MgCl₂, 0.05mM MnCl₂, 0.05mM CoCl₂, 0.004mM FeSO₄, 5mM Cysteine, 20mM NaHCO₃, 20mM NH₄Cl, 1.2mg/mL Hemin, 1mg/mL menadione, 2mg/mL folic acid, 2mg/mL cobalamine, 10mM acetate, 0.2% BME vitamins, and 20mM glucose. Epsilon medium has the same composition as gamma medium, but also contains 1% Tryptone. All bacteria were cultured in glass tubes in anaerobic work benches, in temperature controlled dry baths at 37°C, shaking with 450rpm. Cultures were inoculated from glycerol stocks stored at -80°C, which were transferred to the anaerobic work benches before opening.

Growth experiments and sampling for metabolite analysis. For growth experiments, glycerol stocks of bacterial cells were taken from a -80°C freezer to an anaerobic workbench. Cells were then transferred from stocks to sterile glass tubes with YCA or BHIS media (seeding culture). After substantial growth, as indicated by an optical density at 600nm (OD_{600}) over 0.1, cultures were diluted into new culture tubes with YCA (pre-culture). Before cells reached saturation, $OD_{600} < 1$, cultures were then diluted again into fresh media to $OD_{600} \approx 0.02$ to start the experimental cultures. Growth was then tracked by regular measurements of OD_{600} (around 7 measurements between OD_{600} 0.05 and 0.5). OD_{600} measurements were performed in Quartz semi-micro-cuvettes in a benchtop spectrophotometer or by directly determining optical density of the culture tubes. We also collected four to six samples of 200 μ l culture volume for the subsequent quantification of sugar and fermentation products concentrations. These samples were transferred to sterile 0.2 μ m filter centrifuge tubes, and centrifuged at 11'000g for 2min to remove cells. Samples were then kept at 4°C until further analysis. For all samples, optical densities were typically kept between $OD_{600} \approx 0.04$ to 0.5 to ensure linearity between absorbance and bacterial biomass. These measurements were done in YCA, BHIS, epsilon, and gamma media, typically for three biological replicates each. Depending on the medium used, not all strains were able to grow and we report only results for strains which showed substantial growth in the respective media. Media compositions are provided above.

Chromatography Method to Determine Nutrient Uptake and Fermentation Product Secretion. Metabolite concentrations in filtered samples from culture supernatants were analyzed using isocratic HPLC with refractive index detection (RID), as described in (11). In short, 20 μ l of sample was injected using an autosampler cooled to 10°C, separated over an ion exchange column (Phenomenex Rezex RoA organic acid H⁺ (8%), LC column 300 x 7.8mm) in a column oven at 40°C, at a flow rate of 0.4ml/min, with 2.5mM H₂SO₄ in water as mobile phase. Chromatography data from the RID detector was recorded for 40min, exported as plain text files, and analyzed using custom Python scripts which has subsequently been

released as a standalone software package (57). An example of the analysis is discussed in **Figure S1** and the analysis scripts are available on the GitHub repository of this study. In short, a background correction based on the algorithm described in (58) was applied and areas under all the peaks representing the metabolites of interest were extracted. These areas were compared to a standard curve of known metabolite concentrations, and values for uptake or excretion per biomass were then calculated for every growth experiment.

Estimate daily fermentation product release: To calculate the daily release of fermentation bacteria in the large intestine we started with estimations on the bacterial biomass released daily in feces $M_{fec,bac}$, or the daily amount of complex carbohydrates which reach the large intestine and are digestible by bacteria, M_{carb} . These values either follow from fecal mass measurements more direct characterizations of luminal content, or from a mapping estimating the link between consumed carbohydrates and those available for the microbiota to utilize. We then calculated the daily release as $FP_{tot} = \epsilon_{tot} \cdot M_{bact}$ or $FP_{tot} = \epsilon_{tot} \cdot Y_{carb} \cdot M_{carb}$, were we took the average of the excretion and yield values measured for all strains. Full details of this approach are provided in **SI Text 3**. To account for variations in microbiome composition, we further weighted the values of different strains based on their metabolically determined relative abundance in different samples covering different studies from the curated metagenomic dataset (25). Full details of this approach are described in **SI Text 6** and results for different studies are shown in the **Interactive Figure 1**.

Calculation of variation with diet. To obtain variations with diet, we analyzed different datasets on dietary composition and fecal weight as introduced. From dietary data we estimated the variation in microbiota available carbohydrates which we then used to calculate the variation in the daily release of FP using the via-carbohydrate estimation (**Figures 2BC and S8, SI Text 3**). From fecal wet weight data we estimated the variation of daily bacterial biomass released in feces, accounting for changes in fecal water uptake (**Figure S9**). With this data we then calculated the daily FP release using the via-feces estimation (**Figure 2A and SI Text 3**).

Code and Data Availability

All Python code, raw chromatograms and processed data are available on the paper's GitHub repository (<https://doi.org/10.5281/zenodo.10445504>) accessible via the website https://github.com/cremerlab/fermentation_products. Interactive figures are available at https://cremerlab.github.io/fermentation_products/study-explorer.

Acknowledgements

We thank Daniel Hoces, Verena Lentsch, Anna Sintsova, Alfred Spormann, and all members of the Cremer, Spormann, and Slack groups for suggestions and discussions.

Funding

MA and ES were supported as a part of NCCR Microbiomes, a National Centre of Competence in Research, funded by the Swiss National Science Foundation (grant number 180575), and by project grants from the Swiss National Science Foundation (grant numbers 40B2-0_180953, 310030_185128). CM was supported by an Innosuisse grant (grant number 59256.1 IP-LS). GC was supported by the NSF Postdoctoral Research Fellowships in Biology

Program (grant number 2010807). ES was also supported by the Botnar Research Centre for Child Health as part of the Multi-Investigator Project: Microbiota Engineering for Child Health. JC acknowledges support by a Stanford Bio-X Seeding Grant (grant number 10-32) and a Terman fellowship.

References

1. B. Dalile, L. Van Oudenhove, B. Vervliet, K. Verbeke, The role of short-chain fatty acids in microbiota–gut–brain communication. *Nat. Rev. Gastroenterol. Hepatol.* **16**, 461–478 (2019).
2. A. Koh, F. D. Vadder, P. Kovatcheva-Datchary, F. Bäckhed, From Dietary Fiber to Host Physiology: Short-Chain Fatty Acids as Key Bacterial Metabolites. *Cell* **165**, 1332–1345 (2016).
3. P. J. Turnbaugh, R. E. Ley, M. A. Mahowald, V. Magrini, E. R. Mardis, J. I. Gordon, An obesity-associated gut microbiome with increased capacity for energy harvest. *Nature* **444**, 1027–1031 (2006).
4. V. K. Ridaura, J. J. Faith, F. E. Rey, J. Cheng, A. E. Duncan, A. L. Kau, N. W. Griffin, V. Lombard, B. Henrissat, J. R. Bain, M. J. Muehlbauer, O. Ilkayeva, C. F. Semenkovich, K. Funai, D. K. Hayashi, B. J. Lyle, M. C. Martini, L. K. Ursell, J. C. Clemente, W. V. Treuren, W. A. Walters, R. Knight, C. B. Newgard, A. C. Heath, J. I. Gordon, Gut microbiota from twins discordant for obesity modulate metabolism in mice. *Science* **341**, 1241214–1241214 (2013).
5. R. Corrêa-Oliveira, J. L. Fachi, A. Vieira, F. T. Sato, M. A. R. Vinolo, Regulation of immune cell function by short-chain fatty acids. *Clin. Transl. Immunol.* **5**, e73 (2016).
6. Y. Furusawa, Y. Obata, S. Fukuda, T. A. Endo, G. Nakato, D. Takahashi, Y. Nakanishi, C. Uetake, K. Kato, T. Kato, M. Takahashi, N. N. Fukuda, S. Murakami, E. Miyauchi, S. Hino, K. Atarashi, S. Onawa, Y. Fujimura, T. Lockett, J. M. Clarke, D. L. Topping, M. Tomita, S. Hori, O. Ohara, T. Morita, H. Koseki, J. Kikuchi, K. Honda, K. Hase, H. Ohno, Commensal microbe-derived butyrate induces the differentiation of colonic regulatory T cells. *Nature*, 1–8 (2013).
7. C. Schneider, C. E. O’Leary, J. von Moltke, H.-E. Liang, Q. Y. Ang, P. J. Turnbaugh, S. Radhakrishnan, M. Pellizzon, A. Ma, R. M. Locksley, A Metabolite-Triggered Tuft Cell-ILC2 Circuit Drives Small Intestinal Remodeling. *Cell* **174**, 271-284.e14 (2018).
8. G. Frost, M. L. Sleeth, M. Sahuri-Arisoylu, B. Lizarbe, S. Cerdan, L. Brody, J. Anastasovska, S. Ghourab, M. Hankir, S. Zhang, D. Carling, J. R. Swann, G. Gibson, A. Viardot, D. Morrison, E. Louise Thomas, J. D. Bell, The short-chain fatty acid acetate reduces appetite via a central homeostatic mechanism. *Nat. Commun.* **5**, 3611 (2014).
9. C. Torres-Fuentes, H. Schellekens, T. G. Dinan, J. F. Cryan, The microbiota-gut-brain axis in obesity. *Lancet Gastroenterol. Hepatol.* **2**, 747–756 (2017).
10. F. De Vadder, E. Grasset, L. Mannerås Holm, G. Karsenty, A. J. Macpherson, L. E. Olofsson, F. Bäckhed, Gut microbiota regulates maturation of the adult enteric nervous system via enteric serotonin networks. *Proc. Natl. Acad. Sci. U. S. A.* **115**, 6458–6463 (2018).
11. J. Cremer, M. Arnoldini, T. Hwa, Effect of water flow and chemical environment on microbiota growth and composition in the human colon. *Proc. Natl. Acad. Sci. U. S. A.* **114**, 6438–6443 (2017).

12. A. W. Walker, S. H. Duncan, E. C. M. Leitch, M. W. Child, H. J. Flint, pH and Peptide Supply Can Radically Alter Bacterial Populations and Short-Chain Fatty Acid Ratios within Microbial Communities from the Human Colon. *Appl. Environ. Microbiol.* **71**, 3692–3700 (2005).
13. J. H. Cummings, H. N. Englyst, Fermentation in the human large intestine and the available substrates. *Am. J. Clin. Nutr.* **45**, 1243–1255 (1987).
14. J. H. Cummings, M. J. Hill, D. J. Jenkins, J. R. Pearson, H. S. Wiggins, Changes in fecal composition and colonic function due to cereal fiber. *Am. J. Clin. Nutr.* **29**, 1468–1473 (1976).
15. S. F. Phillips, J. Giller, The contribution of the colon to electrolyte and water conservation in man. *J. Lab. Clin. Med.* **81**, 733–746 (1973).
16. D. Hoces, J. Lan, W. Sun, T. Geiser, M. L. Stäubli, E. Cappio Barazzone, M. Arnoldini, T. D. Challa, M. Klug, A. Kellenberger, S. Nowok, E. Faccin, A. J. Macpherson, B. Stecher, S. Sunagawa, R. Zenobi, W.-D. Hardt, C. Wolfrum, E. Slack, Metabolic reconstitution of germ-free mice by a gnotobiotic microbiota varies over the circadian cycle. *PLOS Biol.* **20**, e3001743 (2022).
17. J. Lloyd-Price, C. Arze, A. N. Ananthakrishnan, M. Schirmer, J. Avila-Pacheco, T. W. Poon, E. Andrews, N. J. Ajami, K. S. Bonham, C. J. Brislawn, D. Casero, H. Courtney, A. Gonzalez, T. G. Graeber, A. B. Hall, K. Lake, C. J. Landers, H. Mallick, D. R. Plichta, M. Prasad, G. Rahnavard, J. Sauk, D. Shungin, Y. Vázquez-Baeza, R. A. White, J. Braun, L. A. Denson, J. K. Jansson, R. Knight, S. Kugathasan, D. P. B. McGovern, J. F. Petrosino, T. S. Stappenbeck, H. S. Winter, C. B. Clish, E. A. Franzosa, H. Vlamakis, R. J. Xavier, C. Huttenhower, Multi-omics of the gut microbial ecosystem in inflammatory bowel diseases. *Nature* **569**, 655–662 (2019).
18. M. Schirmer, E. A. Franzosa, J. Lloyd-Price, L. J. McIver, R. Schwager, T. W. Poon, A. N. Ananthakrishnan, E. Andrews, G. Barron, K. Lake, M. Prasad, J. Sauk, B. Stevens, R. G. Wilson, J. Braun, L. A. Denson, S. Kugathasan, D. P. B. McGovern, H. Vlamakis, R. J. Xavier, C. Huttenhower, Dynamics of metatranscription in the inflammatory bowel disease gut microbiome. *Nat. Microbiol.* **3**, 337–346 (2018).
19. N. I. McNeil, The contribution of the large intestine to energy supplies in man. *Am. J. Clin. Nutr.* **39**, 338–342 (1984).
20. J. B. Wyman, K. W. Heaton, A. P. Manning, A. C. Wicks, Variability of colonic function in healthy subjects. *Gut* **19**, 146–150 (1978).
21. A. M. Stephen, J. H. Cummings, The Microbial Contribution to Human Fecal Mass. *J. Med. Microbiol.* **13**, 45–56 (1980).
22. *Household Food Consumption and Expenditure: Annual Report of the National Food Survey Committee* (H.M.S.O., ed. 1976) (1976).
23. T. Høverstad, O. Fausa, A. Bjørneklett, T. Bøhmer, Short-Chain Fatty Acids in the Normal Human Feces. *Scand. J. Gastroenterol.* **19**, 375–381 (1984).
24. The Integrative HMP (iHMP) Research Network Consortium, The Integrative Human Microbiome Project. *Nature* **569**, 641–648 (2019).

25. E. Pasolli, L. Schiffer, P. Manghi, A. Renson, V. Obenchain, D. T. Truong, F. Beghini, F. Malik, M. Ramos, J. B. Dowd, C. Huttenhower, M. Morgan, N. Segata, L. Waldron, Accessible, curated metagenomic data through ExperimentHub. *Nat. Methods* **14**, 1023–1024 (2017).
26. M. Heldal, S. Norland, O. Tumyr, X-ray microanalytic method for measurement of dry matter and elemental content of individual bacteria. *Appl. Environ. Microbiol.* **50**, 1251–1257 (1985).
27. *National Health and Nutrition Examination Survey (NHANES) Data 2017-2018* (Centers for Disease Control and Prevention (CDC). National Center for Health Statistics (NCHS), Hyattsville, MD: US Department of Health and Human Services) (2018).
28. S. J. D. O'Keefe, J. V. Li, L. Lahti, J. Ou, F. Carbonero, K. Mohammed, J. M. Posma, J. Kinross, E. Wahl, E. Ruder, K. Vipperla, V. Naidoo, L. Mtshali, S. Tims, P. G. B. Puylaert, J. DeLany, A. Krasinskas, A. C. Benefiel, H. O. Kaseb, K. Newton, J. K. Nicholson, W. M. de Vos, H. R. Gaskins, E. G. Zoetendal, Fat, fibre and cancer risk in African Americans and rural Africans. *Nat. Commun.* **6**, 6342–14 (2015).
29. A. L. Kau, P. P. Ahern, N. W. Griffin, A. L. Goodman, J. I. Gordon, Human nutrition, the gut microbiome and the immune system. *Nature* **474**, 327–336 (2011).
30. E. D. Sonnenburg, J. L. Sonnenburg, Starving our Microbial Self: The deleterious consequences of a diet deficient in microbiota-accessible carbohydrates. *Cell Metab.* **20**, 779–786 (2014).
31. H. Pontzer, B. M. Wood, Effects of Evolution, Ecology, and Economy on Human Diet: Insights from Hunter-Gatherers and Other Small-Scale Societies. *Annu. Rev. Nutr.* **41**, 363–385 (2021).
32. F. W. Marlowe, J. C. Berbesque, Tubers as fallback foods and their impact on Hadza hunter-gatherers. *Am. J. Phys. Anthropol.* **140**, 751–758 (2009).
33. D. P. Burkitt, A. R. P. Walker, N. S. Painter, Effect of Dietary Fibre on Stools and Transit-Times, and its Role in the Causation of Disease. *The Lancet* **300**, 1408–1411 (1972).
34. A. M. Stephen, J. H. Cummings, Mechanism of action of dietary fibre in the human colon. *Nature* **284**, 283–284 (1980).
35. C. J. Prynne, D. A. T. Southgate, The effects of a supplement of dietary fibre on faecal excretion by human subjects. *Br. J. Nutr.* **41**, 495–503 (1979).
36. J. H. Cummings, M. J. Hill, T. Jivraj, H. Houston, W. J. Branch, D. J. A. Jenkins, The effect of meat protein and dietary fiber on colonic function and metabolism I. Changes in bowel habit, bile acid excretion, and calcium absorption. *Am. J. Clin. Nutr.* **32**, 2086–2093 (1979).
37. R. L. Walters, I. M. Baird, P. S. Davies, M. J. Hill, B. S. Drasar, D. A. Southgate, J. Green, B. Morgan, Effects of two types of dietary fibre on faecal steroid and lipid excretion. *BMJ* **2**, 536–538 (1975).
38. A. M. Stephen, H. S. Wiggins, H. N. Englyst, T. J. Cole, B. J. Wayman, J. H. Cummings, The effect of age, sex and level of intake of dietary fibre from wheat on large-bowel function in thirty healthy subjects. *Br. J. Nutr.* **56**, 349–361 (1986).

39. D. P. Burkitt, *Don't Forget Fibre in Your Diet* (CRC Press, ed. 1) (2004).
40. FAO, Human energy requirements. Report of a Joint FAO/WHO/UNU Expert Consultation (2001).
41. G. Porter, M. Festing, A comparison between irradiated and autoclaved diets for breeding mice, with observations on palatability. *Lab. Anim.* **4**, 203–213 (1970).
42. R. Sender, S. Fuchs, R. Milo, Revised Estimates for the Number of Human and Bacteria Cells in the Body. *PLOS Biol.* **14**, e1002533 (2016).
43. A. W. Walker, L. Hoyles, Human microbiome myths and misconceptions. *Nat. Microbiol.* **8**, 1392–1396 (2023).
44. G. den Besten, K. van Eunen, A. K. Groen, K. Venema, D.-J. Reijngoud, B. M. Bakker, The role of short-chain fatty acids in the interplay between diet, gut microbiota, and host energy metabolism. *J. Lipid Res.* **54**, 2325–2340 (2013).
45. L. A. David, C. F. Maurice, R. N. Carmody, D. B. Gootenberg, J. E. Button, B. E. Wolfe, A. V. Ling, A. S. Devlin, Y. Varma, M. A. Fischbach, S. B. Biddinger, R. J. Dutton, P. J. Turnbaugh, Diet rapidly and reproducibly alters the human gut microbiome. *Nature* **505**, 559–563 (2014).
46. F. Hugenholz, W. M. de Vos, Mouse models for human intestinal microbiota research: a critical evaluation. *Cell. Mol. Life Sci.* **75**, 149–160 (2017).
47. R. Lundberg, Humanizing the gut microbiota of mice: Opportunities and challenges. *Lab. Anim.* **53**, 244–251 (2019).
48. D. Masopust, C. P. Sivula, S. C. Jameson, Of Mice, Dirty Mice, and Men: Using Mice To Understand Human Immunology. *J. Immunol.* **199**, 383–388 (2017).
49. T. L. A. Nguyen, S. Vieira-Silva, A. Liston, J. Raes, How informative is the mouse for human gut microbiota research? *Dis. Model. Mech.* **8**, 1–16 (2015).
50. J. Walter, A. M. Armet, B. B. Finlay, F. Shanahan, Establishing or Exaggerating Causality for the Gut Microbiome: Lessons from Human Microbiota-Associated Rodents. *Cell* **180**, 221–232 (2020).
51. R. F. McLoughlin, B. S. Berthon, M. E. Jensen, K. J. Baines, L. G. Wood, Short-chain fatty acids, prebiotics, synbiotics, and systemic inflammation: a systematic review and meta-analysis. *Am. J. Clin. Nutr.*, ajcn156265 (2017).
52. O. Wrong, Nitrogen metabolism in the gut. *Am. J. Clin. Nutr.* **31**, 1587–1593 (1978).
53. N. Nakamura, H. C. Lin, C. S. McSweeney, R. I. Mackie, H. R. Gaskins, Mechanisms of Microbial Hydrogen Disposal in the Human Colon and Implications for Health and Disease. *Annu. Rev. Food Sci. Technol.* **1**, 363–395 (2010).
54. J. Cremer, I. Segota, C. Yang, M. Arnoldini, J. T. Sauls, Z. Zhang, E. Gutierrez, A. Groisman, T. Hwa, Effect of flow and peristaltic mixing on bacterial growth in a gut-like channel. *Proc. Natl. Acad. Sci. U. S. A.* **113**, 11414–11419 (2016).
55. L. V. Holdeman, W. E. C. Moore, E. P. Cato, *Anaerobe Laboratory Manual*. Va. *Polytech. Inst. State Univ. Anaerobe Lab.* (1977).

56. S. H. Duncan, P. Louis, J. M. Thomson, H. J. Flint, The role of pH in determining the species composition of the human colonic microbiota. *Environ. Microbiol.* **11**, 2112–2122 (2009).
57. G. Chure, J. Cremer, hplc-py: A Python Package For Rapid Peak Quantification in Complex Chromatograms. *chemRxiv*. (2023).
58. M. Morháč, V. Matoušek, Peak Clipping Algorithms for Background Estimation in Spectroscopic Data. *Appl. Spectrosc.* **62**, 91–106 (2008).